Computers & Structures Vol. 31, No. 4, pp. 553–565, 1989
Printed in Great Britain.

0045-7949/89 $3.00 + 0.00

PLANE STRESS ANALYSIS USING MACRO ELEMENTS

J. PETROLITO and B. W. GOLLEY
Department of Civil Engineering, University College, Australian Defence Force Academy, Campbell, ACT, Australia

(*Received* 19 *February* 1988)

Abstract—A variable degree of freedom plane stress element is presented. The displacement functions within an element satisfy the governing equations of elasticity, substantially reducing the number of equations requiring generation and solution for the accurate analysis of two-dimensional stress problems. Large elements may be used, requiring a minimum of data preparation. The examples considered show that engineering accuracy may be obtained with the generation and solution of very few equations.

INTRODUCTION

Two-dimensional stress analysis of structures with complicated boundaries requires that the region to be analysed should be divided into a large number of elements. This leads to a large number of equations requiring solution for accurate results. Triangular or isoparametric elements are required to adequately define the boundary. However, many commonly occurring structures can be conveniently discretized using rectangular elements, and high-order finite elements have recently been proposed for shear wall analysis [1] and deep beam analysis [2].

The term macro element has been used to describe a finite element suitable for modelling a domain with minimum discretization. In this paper, a variable degree of freedom rectangular macro element is presented for use in two-dimensional stress analysis. The element may be combined with an analogous plate bending macro element [3], enabling fully composite beam–slab systems to be efficiently analysed [4]. In addition, the techniques described in [5, 6] may be used to enable more general geometries to be treated. The element formulation parallels that used for the development of the analogous plate bending macro element [3].

TWO-DIMENSIONAL ELASTICITY THEORY

The usual assumptions of two-dimensional elasticity theory apply [7]. With the notation of Fig. 1, the two equilibrium equations are

$$\mathbf{D}\boldsymbol{\sigma} + \bar{\mathbf{b}} = \mathbf{0}, \tag{1}$$

where $\boldsymbol{\sigma} = \lfloor \sigma_{xx} \quad \sigma_{yy} \quad \sigma_{xy} \rfloor^T$, $\bar{\mathbf{b}} = \lfloor \bar{b}_x \quad \bar{b}_y \rfloor^T$ and

$$\mathbf{D} = \begin{bmatrix} \partial/\partial x & 0 & \partial/\partial y \\ 0 & \partial/\partial y & \partial/\partial x \end{bmatrix}. \tag{2}$$

The stresses are related to the displacements, u and v, by

$$\boldsymbol{\sigma} = \mathbf{E}\mathbf{D}^T\mathbf{u} \tag{3}$$

where $\mathbf{u} = \lfloor u \quad v \rfloor^T$ and $\mathbf{E}$ is a matrix of material properties. For an isotropic material under plane stress conditions

$$\mathbf{E} = \frac{E}{1-\nu^2}\begin{bmatrix} 1 & \nu & 0 \\ \nu & 1 & 0 \\ 0 & 0 & (1-\nu)/2 \end{bmatrix}, \tag{4}$$

where E is Young's modulus and ν is Poisson's ratio. The plane strain equations are analogous and are not repeated here. Any plane strain problem can be treated as an analogous plane stress problem by suitably adjusting the material properties [7].

ELEMENT DISPLACEMENT FUNCTIONS

In a typical element, e, shown in Fig. 2, the displacements are approximated by

$$u^e = \mathbf{N}_p^e(x,y)\boldsymbol{\phi}_p^e + \sum_{m=1}^{M} \mathbf{N}_{lm}^e(x,y)\boldsymbol{\phi}_{lm}^e + \sum_{m=1}^{M^*} \mathbf{N}_{nm}^e(x,y)\boldsymbol{\phi}_{nm}^e + u_o^e(x,y)$$

$$v = \bar{\mathbf{N}}_p^e(x,y)\boldsymbol{\phi}_p^e + \sum_{m=1}^{M} \bar{\mathbf{N}}_{lm}^e(x,y)\boldsymbol{\phi}_{lm}^e + \sum_{m=1}^{M^*} \bar{\mathbf{N}}_{nm}^e(x,y)\boldsymbol{\phi}_{nm}^e + v_o^e(x,y) \tag{5}$$

or

$$u^e = u_p^e + u_l^e + u_n^e + u_o^e$$

$$v^e = v_p^e + v_l^e + v_n^e + v_o^e \tag{6}$$

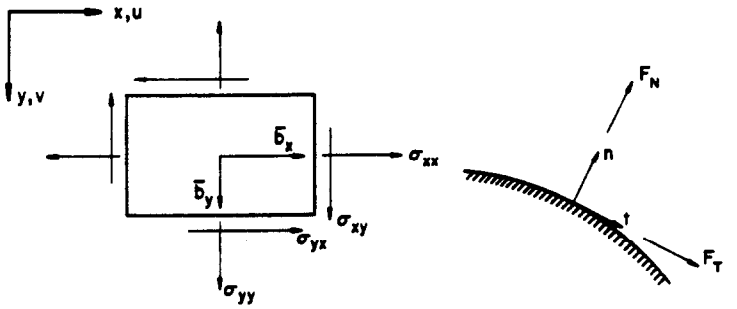

Fig. 1. Sign convention.

The terms in eqn. (5) are obtained by the superposing of the four cases shown in Fig. 3.

The first terms for u^e and v^e in eqn. (5) are derived as follows. The displacements, u_p^e and v_p^e, within the element are taken as the polynomial functions

$$u_p^e = \mathbf{P}(x, y)\mathbf{A}^e$$

$$v_p^e = \tilde{\mathbf{P}}(x, y)\mathbf{A}^e, \tag{7}$$

where the matrices $\mathbf{P}$ and $\tilde{\mathbf{P}}$ contain polynomial functions which satisfy the homogeneous form (i.e. $\bar{\mathbf{b}} = \mathbf{0}$) of eqn. (1) and $\mathbf{A}^e$ is a matrix of parameters. The terms in $\mathbf{P}$ and $\tilde{\mathbf{P}}$ may be obtained using either a complex variable approach [8] or the procedure developed in [4], and are given in the Appendix. The element degrees of freedom (see Fig. 3a),

$$\boldsymbol{\phi}_p^e = \{u_1^e \; v_1^e \; u_2^e \; u_3^e \; v_3^e \; v_4^e \; u_5^e \; v_5^e \; u_6^e \; u_7^e \; v_7^e \; v_8^e\} \tag{8}$$

are the displacements at the corner and midside nodes. The midside variables are common to adjacent elements while the corner variables are local to the element. $\boldsymbol{\phi}_p^e$ is expressed in terms of $\mathbf{A}^e$ as

$$\boldsymbol{\phi}_p^e = \mathbf{C}^e\mathbf{A}^e. \tag{9}$$

Combining eqns (7) and (9) gives

$$u_p^e = \mathbf{P}(x, y)(\mathbf{C}^e)^{-1}\boldsymbol{\phi}_p^e = \mathbf{N}_p^e(x, y)\boldsymbol{\phi}_p^e$$

$$v_p^e = \tilde{\mathbf{P}}(x, y)(\mathbf{C}^e)^{-1}\boldsymbol{\phi}_p^e = \tilde{\mathbf{N}}_p^e(x, y)\boldsymbol{\phi}_p^e. \tag{10}$$

The terms in $\mathbf{N}_p^e$ and $\tilde{\mathbf{N}}_p^e$ have been evaluated explicitly and are given in the Appendix.

During the elimination of the corner displacements, which is discussed later, the first terms in eqn. (10) are required in partitioned form, namely

$$u_p^e = \lfloor \mathbf{N}_{p1}^e \quad \mathbf{N}_{p2}^e \rfloor \begin{Bmatrix} \boldsymbol{\phi}_{p1}^e \\ \boldsymbol{\phi}_{p2}^e \end{Bmatrix}$$

$$v_p^e = \lfloor \tilde{\mathbf{N}}_{p1}^e \quad \tilde{\mathbf{N}}_{p2}^e \rfloor \begin{Bmatrix} \boldsymbol{\phi}_{p1}^e \\ \boldsymbol{\phi}_{p2}^e \end{Bmatrix}, \tag{11}$$

where

$$\boldsymbol{\phi}_{p1}^e = \{u_2^e \; v_4^e \; u_6^e \; v_8^e\}$$

$$\boldsymbol{\phi}_{p2}^e = \{u_1^e \; v_1^e \; u_3^e \; v_3^e \; u_5^e \; v_5^e \; u_7^e \; v_7^e\}. \tag{12}$$

The second terms for u^e and v^e in eqn. (5) result from the application of boundary tangential displacements as shown in Fig. 3(b), with boundary normal

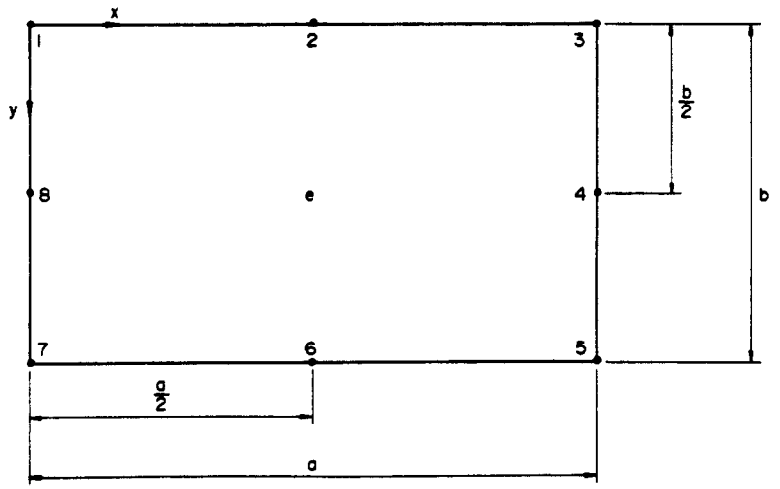

Fig. 2. Typical macro element.

stresses zero. The boundary tangential displacements on the sides of the element are approximated by truncated cosine series, i.e.

$$u_i^e(x,0) = \sum_{m=1}^{M} \phi_{im13}^e \cos(\alpha_m x)$$

$$v_i^e(a,y) = \sum_{m=1}^{M} \phi_{im35}^e \cos(\beta_m y)$$

$$u_i^e(x,b) = \sum_{m=1}^{M} \phi_{im57}^e \cos(\alpha_m x)$$

$$v_i^e(0,y) = \sum_{m=1}^{M} \phi_{im17}^e \cos(\beta_m y), \qquad (13)$$

where $\alpha_m = m\pi/a$ and $\beta_m = m\pi/b$. The coefficients $\phi_{im13}^e, \ldots, \phi_{im17}^e$ are common to adjacent elements. The subscripts 13, 35, etc., refer to sides between corner nodes 1 and 3, 3 and 5, etc. The upper limits of the series in eqn. (13) may in general vary on different sides of the element. This would lead to computational efficiency in some cases. However, for simplicity, it is assumed that the same number of terms is taken on each side of the element.

With boundary tangential displacements specified by eqn. (13) and with normal stresses zero on the boundary of the element, solutions of the homogeneous form of eqn. (1) are obtained in terms of the coefficients ϕ_{im13}^e, ϕ_{im35}^e, ϕ_{im57}^e and ϕ_{im17}^e. These

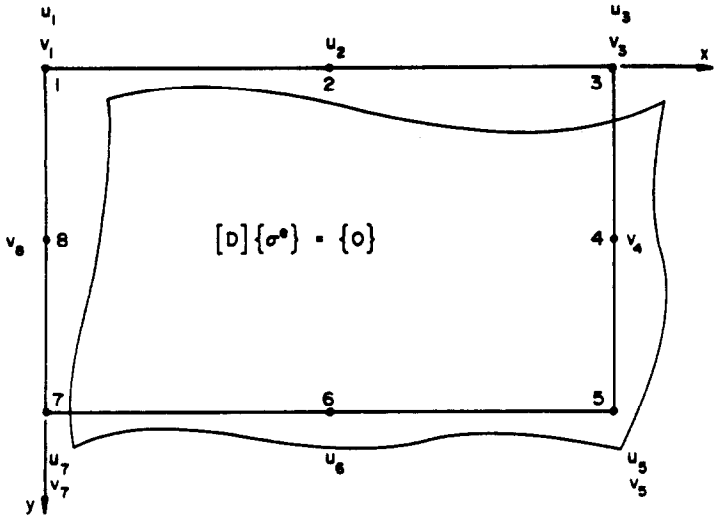

Fig. 3(a).

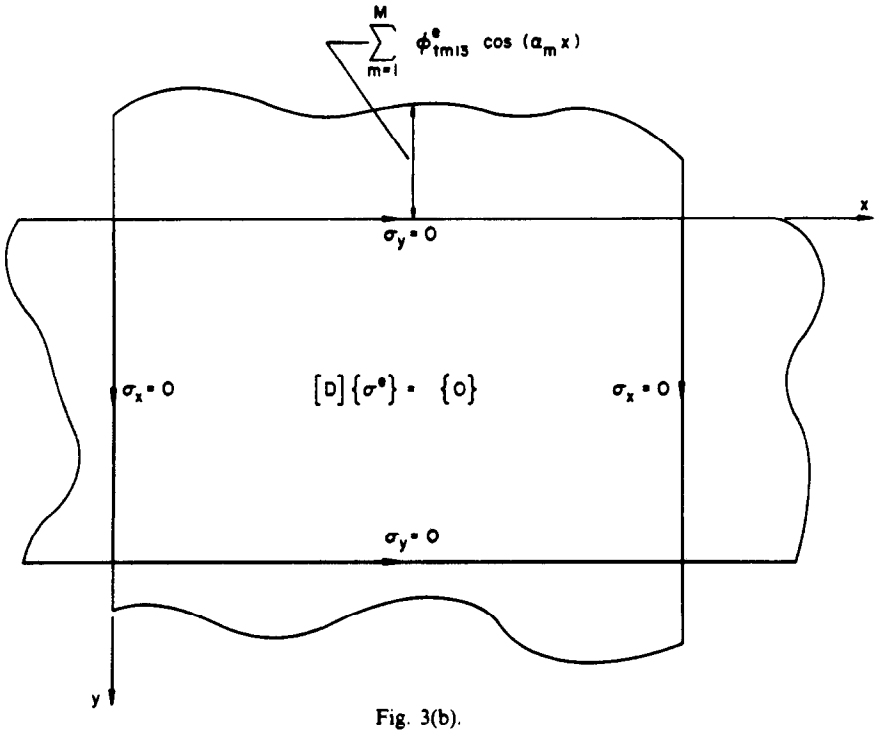

Fig. 3(b).

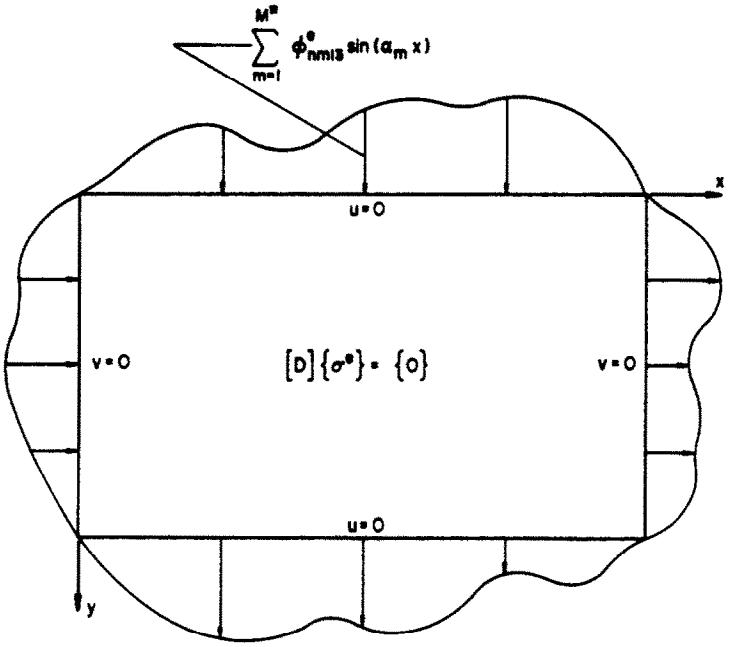

Fig. 3(c).

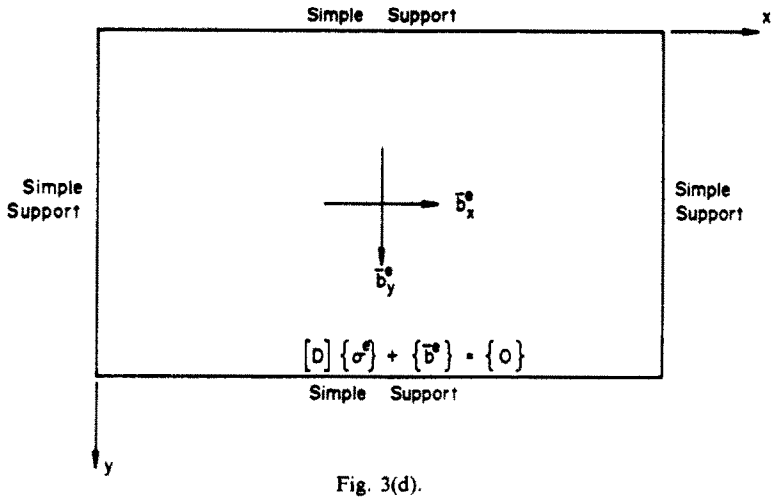

Fig. 3(d).

Fig. 3. Displacement approximations within element. (a) Polynomial terms. (b) Series displacement terms. (c) Series stress terms. (d) Particular solution for specified body loading.

solutions may be obtained using the approach of [9]. Hence for the mth term in the series, the displacements are given by

$$u^e_{im} = \mathbf{N}^e_{im}(x, y)\boldsymbol{\phi}^e_{im}$$
$$v^e_{im} = \tilde{\mathbf{N}}^e_{im}(x, y)\boldsymbol{\phi}^e_{im}, \tag{14}$$

where

$$\boldsymbol{\phi}^e_{im} = \{\phi^e_{im13} \quad \phi^e_{im35} \quad \phi^e_{im57} \quad \phi^e_{im17}\}. \tag{15}$$

The terms in $\mathbf{N}^e_{im}$ and $\tilde{\mathbf{N}}^e_{im}$ are given in the Appendix. Summing the solutions in eqn. (14) for $m = 1, 2 \ldots M$ gives the second terms for u^e and v^e in eqn. (5).

The third terms for u^e and v^e in eqn. (5) are the displacements due to the application of normal stresses in the form of truncated sine series with zero boundary tangential displacements as shown in Fig. 3(c). On the sides of the element, the normal stresses are approximated by

$$\sigma^e_{yym}(x, 0) = -\sum_{m=0}^{M^e} \phi^e_{nm13} \sin(\alpha_m x)$$
$$\sigma^e_{xxn}(a, y) = \sum_{m=1}^{M^e} \phi^e_{nm35} \sin(\beta_m y)$$
$$\sigma^e_{yym}(x, b) = \sum_{m=1}^{M^e} \phi^e_{nm57} \sin(\alpha_m x)$$
$$\sigma^e_{xxn}(0, y) = -\sum_{m=1}^{M^e} \phi^e_{nm17} \sin(\beta_m y). \tag{16}$$

The coefficients $\phi^e_{nm13}, \ldots, \phi^e_{nm17}$ are not common to adjacent elements. The number of terms in the series in eqn. (16) is taken to be the same on all sides of the element but need not be equal to the number of terms in eqn. (13). The signs in eqn. (16) have been chosen to simplify the formulation of the element stiffness matrix as shown later.

With boundary normal stresses specified by eqn. (16) and with boundary tangential displacements zero, solutions of the homogeneous form of eqn. (1) are obtained in terms of the coefficients ϕ^e_{nm13}, ϕ^e_{nm35}, ϕ^e_{nm57} and ϕ^e_{nm17} using the method of [9]. Hence for the mth term in the series, the displacements are given by

$$u^e_{nm} = \mathbf{N}^e_{nm}(x, y)\boldsymbol{\phi}^e_{nm}$$

$$v^e_{nm} = \tilde{\mathbf{N}}_{nm}(x, y)\boldsymbol{\phi}^e_{nm}, \tag{17}$$

where

$$\boldsymbol{\phi}^e_{nm} = \{\phi^e_{nm13} \quad \phi^e_{nm35} \quad \phi^e_{nm57} \quad \phi^e_{nm17}\}. \tag{18}$$

The terms in $\mathbf{N}^e_{nm}$ and $\tilde{\mathbf{N}}^e_{nm}$ are given in the Appendix. Summing the solutions in eqn. (17) for $m = 1, 2 \ldots M^*$ gives the third terms for u^e and v^e in eqn. (5).

The last terms for u^e and v^e in eqn. (5) are particular solutions of the governing equilibrium equations [eqn. (1)] for the applied body forces with all sides of element simply supported (i.e. zero tangential displacement and zero normal stress) as shown in Fig. 3(d). Polynomial solutions can be used for some loading cases, but for the most general loading, series solutions are required [4]. In the case of constant body forces $\bar{b}_x$ and $\bar{b}_y$, the particular solutions are taken as

$$u^e_o = \frac{y(b-y)\bar{b}_x}{E(1+\nu)}$$

$$v^e_o = \frac{x(a-x)\bar{b}_y}{E(1+\nu)}.$$

ESTABLISHMENT OF DISPLACEMENT CONTINUITY

Continuity of displacements is enforced in two stages. First, continuity of displacements is exactly enforced at the element corners by introducing displacement variables which are common to adjacent elements. Element variables $\boldsymbol{\phi}^e_{p2}$ are eliminated at the element level. This step also ensures that tangential displacements are continuous between adjacent elements.

Second, continuity of normal displacements between adjacent elements is approximately established on element sides by introducing new variables which are weighted integrals of side normal displacements. The normal stress variables $\boldsymbol{\phi}^e_{nm}$, which are not common to adjacent elements, are then eliminated.

Establishment of displacement continuity at corners

From eqns (5) and (11), the total displacements at the element corners, $\boldsymbol{\phi}^e_c$, are given by

$$\boldsymbol{\phi}^e_c = \boldsymbol{\phi}^e_{p2} + \sum_{m=1}^{M} \mathbf{T}^e_m \boldsymbol{\phi}^e_{im}, \tag{20}$$

where

$$\boldsymbol{\phi}^e_c = \{\bar{u}^e_1 \quad \bar{v}^e_1 \quad \bar{u}^e_3 \quad \bar{v}^e_3 \quad \bar{u}^e_5 \quad \bar{v}^e_5 \quad \bar{u}^e_7 \quad \bar{v}^e_7\} \tag{21}$$

are the total corner displacements and the terms in the transformation matrix $\mathbf{T}^e_m$ are given in the Appendix. Eliminating the coefficients $\boldsymbol{\phi}^e_{p2}$ using eqn. (20) and substituting into eqn. (5) gives the element displacements as

$$u^e = \lfloor \mathbf{N}^e_{p1} \quad \mathbf{N}^e_{p2} \rfloor \begin{Bmatrix} \boldsymbol{\phi}^e_{p1} \\ \boldsymbol{\phi}^e_c \end{Bmatrix} + \sum_{m=1}^{M} \mathbf{N}^{*e}_{im}\boldsymbol{\phi}^e_{im} + \sum_{m=1}^{M^*} \mathbf{N}^e_{nm}\boldsymbol{\phi}^e_{nm} + u^e_o$$

$$v^e = \lfloor \tilde{\mathbf{N}}^e_{p1} \quad \tilde{\mathbf{N}}^e_{p2} \rfloor \begin{Bmatrix} \boldsymbol{\phi}^e_{p1} \\ \boldsymbol{\phi}^e_c \end{Bmatrix} + \sum_{m=1}^{M} \tilde{\mathbf{N}}^{*e}_{im}\boldsymbol{\phi}^e_{im} + \sum_{m=1}^{M^*} \tilde{\mathbf{N}}^e_{nm}\boldsymbol{\phi}^e_{nm} + v^e_o \tag{22}$$

or

$$u^e = \mathbf{N}^e_p\bar{\boldsymbol{\phi}}^e_p + \sum_{m=1}^{M} \mathbf{N}^{*e}_{im}\boldsymbol{\phi}^e_{im} + \sum_{m=1}^{M^*} \mathbf{N}^e_{nm}\boldsymbol{\phi}^e_{nm} + u^e_o$$

$$v^e = \tilde{\mathbf{N}}^e_p\bar{\boldsymbol{\phi}}^e_p + \sum_{m=1}^{M} \tilde{\mathbf{N}}^{*e}_{im}\boldsymbol{\phi}^e_{im} + \sum_{m=1}^{M^*} \tilde{\mathbf{N}}^e_{nm}\boldsymbol{\phi}^e_{nm} + v^e_o, \tag{23}$$

where

$$\mathbf{N}^{*e}_{im} = \mathbf{N}^e_{im} - \mathbf{N}^e_{p2}\mathbf{T}^e_m$$

$$\tilde{\mathbf{N}}^{*e}_{im} = \tilde{\mathbf{N}}^e_{im} - \tilde{\mathbf{N}}^e_{p2}\mathbf{T}^e_m \tag{24}$$

and

$$\bar{\boldsymbol{\phi}}^e_p = \begin{Bmatrix} \boldsymbol{\phi}^e_{p1} \\ \boldsymbol{\phi}^e_c \end{Bmatrix}. \tag{25}$$

The element displacements given by eqn. (23) ensure continuity of displacements at element corners and continuity of tangential displacements throughout.

Establishment of displacement continuity on sides

Several alternatives are available for establishing continuity of displacements on the sides of adjacent elements. Some of these options are discussed in [3]. In this paper, a technique based on a weighted integral approach is used which is analogous to the procedure used in [3] for the development of a plate bending macro element. The weighted integral

approach highlights the manner in which the continuity of normal displacements is achieved. In this approach, new variables which are weighted integrals of side normal displacements, and are common to adjacent elements, are introduced. By eliminating the element normal stress variables, which are not common to adjacent elements, the total potential energy is obtained in terms of displacement variables only.

ELEMENT FORMULATION

From eqn. (23), the element displacements can be written as

$$u^e = \mathbf{N}^e(x, y)\boldsymbol{\phi}^e + u_o^e(x, y)$$

$$v^e = \tilde{\mathbf{N}}^e(x, y)\boldsymbol{\phi}^e + v_o^e(x, y), \tag{26}$$

where

$$\mathbf{N}^e = \lfloor \mathbf{N}_p^e \quad \mathbf{N}_{t1}^e \quad \mathbf{N}_{t2}^e \quad \dots \quad \mathbf{N}_{tM}^e \quad \mathbf{N}_{n2}^e \quad \dots \quad \mathbf{N}_{nM^e}^e \rfloor$$

$$\tilde{\mathbf{N}}^e = \lfloor \tilde{\mathbf{N}}_p^e \quad \tilde{\mathbf{N}}_{t1}^e \quad \tilde{\mathbf{N}}_{t2}^e \quad \dots \quad \tilde{\mathbf{N}}_{tM}^e \quad \tilde{\mathbf{N}}_{n1}^e \quad \tilde{\mathbf{N}}_{n2}^e \quad \dots \quad \tilde{\mathbf{N}}_{nM^e}^e \rfloor$$

and

$$\boldsymbol{\phi}^e = \{\bar{\boldsymbol{\phi}}_p^e \quad \phi_{t1}^e \quad \phi_{t2}^e \dots \phi_{tM}^e \quad \phi_{n1}^e \quad \phi_{n2}^e \dots \phi_{nM^e}^e\}. \tag{28}$$

To simplify the derivation, it is convenient to work in terms of normal and tangential coordinates (see Fig. 1). Using eqn. (26), the displacements and forces around the boundary of element e can be formally expressed in terms of a tangential coordinate t as

$$u_t^e(t) = \mathbf{N}_{ut}^e(t)\boldsymbol{\phi}^e$$

$$u_n^e(t) = \mathbf{N}_{un}^e(t)\boldsymbol{\phi}^e + u_{no}^e(t)$$

$$F_t^e(t) = \sigma_t^e h^e = \mathbf{N}_{Ft}^e(t)\boldsymbol{\phi}^e + F_{to}^e(t)$$

$$F_n^e(t) = \sigma_n^e h^e = \mathbf{N}_{Fn}^e(t)\boldsymbol{\phi}^e, \tag{29}$$

where σ_t^e and σ_n^e are the stress components in the tangential and normal directions (see Fig. 1), h^e is the thickness of the element and the terms u_{no}^e and F_{to}^e arise from the particular solution for the applied body forces. Since the particular solution is associated with simple supports around the element boundary, there are no particular solution terms for u_t^e and F_n^e.

The total potential energy of the region under analysis is

$$\Pi_p = \sum_e \left(\frac{1}{2} \int_{A^e} \boldsymbol{\sigma}^{eT} \mathbf{D}^T \mathbf{u}^e h^e \, dA - \int_{A^e} \bar{\mathbf{b}}^{eT} \mathbf{u}^e h^e \, dA - \int_{\Gamma_\sigma^e} (\bar{F}_t^e u_t^e + \bar{F}_n^e u_n^e) \, d\Gamma \right), \tag{30}$$

where A^e is the area of element e, Γ_σ^e is the portion of element e where force boundary conditions are specified, and the summation is taken over all elements in the region. As eqn. (1) is satisfied within each element, the area integral in the first term of eqn. (30) can be converted to a boundary integral by the use of Clapeyron's theorem [7], i.e.

$$\int_{A^e} \boldsymbol{\sigma}^{eT} \mathbf{D}^T \mathbf{u}^e h^e \, dA = \int_{A^e} \bar{\mathbf{b}}^{eT} \mathbf{u}^e h^e \, dA + \int_{\Gamma^e} (F_t^e u_t^e + F_n^e u_n^e) \, d\Gamma, \tag{31}$$

where Γ^e is the boundary of the element. Combining eqns (30) and (31) gives

$$\Pi_p = \sum_e \left(-\frac{1}{2} \int_{A^e} \bar{\mathbf{b}}^{eT} \mathbf{u}^e h^e \, dA + \frac{1}{2} \int_{\Gamma^e} (F_t u_t^e + F_n u_n^e) \, d\Gamma - \int_{\Gamma_\sigma^e} (\bar{F}_t^e u_t^e + \bar{F}_n^e u_n^e) \, d\Gamma \right). \tag{32}$$

Substituting eqns (26) and (29) into eqn. (32) gives

$$\Pi_p = \sum_e \left(\tfrac{1}{2} \boldsymbol{\phi}^{eT} \mathbf{K}^e \boldsymbol{\phi}^e - \boldsymbol{\phi}^{eT} \mathbf{R}^e + \text{constant} \right), \tag{33}$$

where

$$\mathbf{K}^e = \int_{\Gamma^e} (\mathbf{N}_{Ft}^{eT} \mathbf{N}_{ut}^e + \mathbf{N}_{Fn}^{eT} \mathbf{N}_{un}^e) \, d\Gamma \tag{34}$$

$$\mathbf{R}^e = \frac{1}{2} \int_{A^e} (\bar{b}_x^e \mathbf{N}^{eT} + \bar{b}_y^e \tilde{\mathbf{N}}^{eT}) h^e \, dA - \frac{1}{2} \int_{\Gamma^e} (F_{to}^e \mathbf{N}_{ut}^{eT} + u_{no}^e \mathbf{N}_{Fn}^{eT}) \, d\Gamma + \int_{\Gamma_\sigma^e} (\bar{F}_t^e \mathbf{N}_{ut}^{eT} + \bar{F}_n^e \mathbf{N}_{un}^{eT}) \, d\Gamma, \tag{35}$$

and the constant arises from terms which only involve the particular solution and is independent of $\boldsymbol{\phi}^e$, $\mathbf{K}^e$ is a symmetrical matrix.

The expression for $\mathbf{R}^e$ in eqn. (35) can be simplified by the use of Betti's theorem [7], which leads to the equation

$$\int_{A^e} (\bar{b}_x^e \mathbf{N}^{eT} + \bar{b}_y^e \tilde{\mathbf{N}}^{eT}) h^e \, dA + \int_{\Gamma^e} F_{to}^e \mathbf{N}_{ut}^{eT} \, d\Gamma = \int_{\Gamma^e} u_{no}^e \mathbf{N}_{Fn}^{eT} \, d\Gamma. \tag{36}$$

Combining eqns (35) and (36) gives

$$\mathbf{R}^e = \int_{A^e} (\bar{b}_x^e \mathbf{N}^{eT} + \bar{b}_y^e \tilde{\mathbf{N}}^{eT}) h^e \, dA - \int_{\Gamma^e} u_{no}^e \mathbf{N}_{Fn}^{eT} \, d\Gamma + \int_{\Gamma_\sigma^e} (\bar{F}_t^e \mathbf{N}_{ut}^{eT} + \bar{F}_n^e \mathbf{N}_{un}^{eT}) \, d\Gamma. \quad (37)$$

The terms in $\mathbf{K}^e$ and $\mathbf{R}^e$ have been evaluated explicitly in order to avoid numerical integration [4]. The terms in $\mathbf{R}^e$ associated with $\boldsymbol{\phi}_p^e$ will contain infinite series terms if the particular solution for the applied body forces within the element is expressed as an infinite series. In the remaining terms of $\mathbf{R}^e$, infinite series terms are avoided by noting certain identities from Betti's theorem.

Neglecting the constant, eqn. (33) can be written in partitioned form as

$$\Pi_p = \sum_e \left(\tfrac{1}{2} \{\boldsymbol{\phi}_i^e \quad \boldsymbol{\phi}_j^e\}^T \begin{bmatrix} \mathbf{K}_{ii}^e & \mathbf{K}_{ij}^e \\ \mathbf{K}_{ij}^{eT} & \mathbf{K}_{jj}^e \end{bmatrix} \begin{Bmatrix} \boldsymbol{\phi}_i^e \\ \boldsymbol{\phi}_j^e \end{Bmatrix} - \{\boldsymbol{\phi}_i^e \quad \boldsymbol{\phi}_j^e\}^T \begin{Bmatrix} \mathbf{R}_i^e \\ \mathbf{R}_j^e \end{Bmatrix} \right), \quad (38)$$

where

$$\boldsymbol{\phi}_i^e = \{\bar{\boldsymbol{\phi}}_p^e \quad \boldsymbol{\phi}_{i1}^e \quad \boldsymbol{\phi}_{i2}^e \ldots \boldsymbol{\phi}_{iM}^e\}$$

$$\boldsymbol{\phi}_j^e = \{\boldsymbol{\phi}_{n1}^e \quad \boldsymbol{\phi}_{n2}^e \ldots \boldsymbol{\phi}_{nM^*}^e\}. \quad (39)$$

To enforce continuity of normal displacements on the sides of adjacent elements, weighted integrals of normal displacements are introduced as follows. On the side $y = 0$ of element e, weighted integrals of the normal displacement, $\boldsymbol{\phi}_{n13m}^e$, are defined as

$$\boldsymbol{\phi}_{n13m}^e = \int_0^a \lambda^e \left(\frac{x}{a}, m\right) \left(v^e(x, 0) - v_1^e \left(1 - \frac{x}{a}\right) - v_3^e \left(\frac{x}{a}\right) \right) dx, \quad (40)$$

where

$$\lambda\left(\frac{x}{a}, m\right) = \left\{ \sin\left(\frac{\pi x}{a}\right) \sin\left(\frac{2\pi x}{a}\right) \ldots \sin\left(\frac{(M^* - 2)\pi x}{a}\right) \times \left(1 - \frac{x}{a}\right)\left(\frac{x}{a}\right) \right\}, \quad M^* > 2$$

$$\lambda\left(\frac{x}{a}, m\right) = \left\{ \left(1 - \frac{x}{a}\right)\left(\frac{x}{a}\right) \right\}, \quad M^* = 2$$

$$\lambda\left(\frac{x}{a}, m\right) = \left\{ \sin\left(\frac{\pi x}{a}\right) \right\}, \quad M^* = 1. \quad (41)$$

In eqn. (40), a linear function of the two end displacements, v_1^e and v_3^e, which are common to adjacent elements, has been subtracted from the total normal displacement on the side. This is not necessary for the development of the element, and the weighted integrals could have alternatively been defined as

$$\boldsymbol{\phi}_{n13m}^e = \int_0^a \lambda^e \left(\frac{x}{a}, m\right) v^e(x, 0) \, dx. \quad (42)$$

The use of either the definition in eqn. (40) or (42) together with the procedure detailed below leads to identical results. However, the definition in eqn. (40) is used in preference since it leads to computational advantages when the element is combined with the analogous plate bending macro element [4].

Following the definition in eqn. (40), weighted integrals of normal displacements on the other three sides of the element are defined as

$$\boldsymbol{\phi}_{n35m}^e = \int_0^b \lambda^e \left(\frac{y}{b}, m\right) \left(u^e(a, y) - u_5^e \left(1 - \frac{y}{b}\right) - u_5^e \left(\frac{y}{b}\right) \right) dy$$

$$\boldsymbol{\phi}_{n57m}^e = \int_0^a \lambda^e \left(\frac{x}{a}, m\right) \left(v^e(x, b) - v_5^e \left(1 - \frac{x}{a}\right) - v_5^e \left(\frac{x}{a}\right) \right) dx$$

$$\boldsymbol{\phi}_{n17m}^e = \int_0^b \lambda^e \left(\frac{y}{b}, m\right) \left(u^e(0, y) - u_1^e \left(1 - \frac{y}{b}\right) - u_1^e \left(\frac{y}{b}\right) \right) dy. \quad (43)$$

Substituting for u^e and v^e from eqn. (26) into eqns (40) and (43) and performing the integrations gives

$$\boldsymbol{\phi}_n^e = \mathbf{W}_i^e \boldsymbol{\phi}_i^e + \mathbf{W}_j^e \boldsymbol{\phi}_j^e + \mathbf{W}_o^e, \quad (44)$$

where

$$\boldsymbol{\phi}_n^e = \{\boldsymbol{\phi}_{n131}^e \quad \boldsymbol{\phi}_{n351}^e \quad \boldsymbol{\phi}_{n571}^e \quad \boldsymbol{\phi}_{n171}^e \ldots \boldsymbol{\phi}_{n13M^*}^e \quad \boldsymbol{\phi}_{n35M^*}^e \quad \boldsymbol{\phi}_{n57M^*}^e \quad \boldsymbol{\phi}_{n17M^*}^e\} \quad (45)$$

and is made common to adjacent elements. Note that the first two number subscripts refer to the side number, and the third number subscript refers to the harmonic number. If $M^* > 2$, $\mathbf{W}_j^e$ contains the first $M^* - 2$ rows and columns of $\mathbf{K}_{jj}^e$ as a submatrix. This is a consequence of the weighting functions chosen in eqns (40) and (43) and the sign convention used in eqn. (16).

As the variable $\boldsymbol{\phi}_j^e$ are local to element e, eqn. (44) can be solved for $\boldsymbol{\phi}_j^e$ to give

$$\boldsymbol{\phi}_j^e = (\mathbf{W}_j^e)^{-1} (\boldsymbol{\phi}_n^e - \mathbf{W}_i^e \boldsymbol{\phi}_i^e - \mathbf{W}_0^e). \quad (46)$$

Substituting for $\boldsymbol{\phi}_j^e$ from eqn. (46) into eqn. (38) and neglecting a further constant gives

$$\Pi_p = \sum_e \left(\tfrac{1}{2} \{\boldsymbol{\phi}_i^e \quad \boldsymbol{\phi}_n^e\}^T \begin{bmatrix} \bar{\mathbf{K}}_{ii}^e & \bar{\mathbf{K}}_{ij}^e \\ \bar{\mathbf{K}}_{ij}^{eT} & \bar{\mathbf{K}}_{jj}^e \end{bmatrix} \begin{Bmatrix} \boldsymbol{\phi}_i^e \\ \boldsymbol{\phi}_n^e \end{Bmatrix} - \{\boldsymbol{\phi}_i^e \quad \boldsymbol{\phi}_n^e\}^T \begin{Bmatrix} \bar{\mathbf{R}}_i^e \\ \bar{\mathbf{R}}_j^e \end{Bmatrix} \right) \quad (47)$$

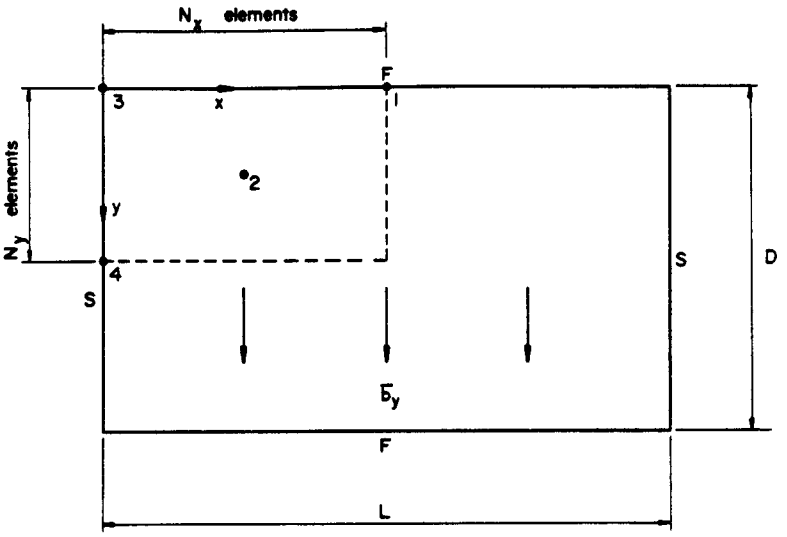

Fig. 4. Example 1: beam subjected to constant body force in y direction.

or

$$\Pi_p = \sum_e \left(\tfrac{1}{2}\bar{\boldsymbol{\phi}}^{eT}\bar{\mathbf{K}}^e\bar{\boldsymbol{\phi}}^{eT} - \bar{\boldsymbol{\phi}}^{eT}\bar{\mathbf{R}}^e\right), \tag{48}$$

where

$$\bar{\mathbf{K}}^e_{ii} = \mathbf{K}^e_{ii} + \mathbf{W}_i^{eT}(\bar{\mathbf{K}}^e_{jj}\mathbf{W}_i^e - (\mathbf{W}_j^e)^{-T}\mathbf{K}_{ij}^{eT}) - \mathbf{K}^e_{ij}(\mathbf{W}_j^e)^{-1}\mathbf{W}_i^e$$

$$\bar{\mathbf{K}}^e_{ij} = \mathbf{K}^e_{ij}(\mathbf{W}_j^e)^{-1} - \mathbf{W}_i^{eT}\bar{\mathbf{K}}^e_{jj}$$

$$\bar{\mathbf{K}}^e_{jj} = (\mathbf{W}_j^e)^{-T}\mathbf{K}^e_{jj}(\mathbf{W}_j^e)^{-1}$$

$$\bar{\mathbf{R}}_i^e = \mathbf{R}_i^e - \mathbf{W}_i^{eT}(\bar{\mathbf{K}}^e_{jj}\mathbf{W}_o^e + (\mathbf{W}_j^e)^{-T}\mathbf{R}_j^e) + \mathbf{K}^e_{ij}(\mathbf{W}_j^e)^{-T}\mathbf{W}_o^e$$

$$\bar{\mathbf{R}}_j^e = \bar{\mathbf{K}}^e_{jj}\mathbf{W}_o^e + (\mathbf{W}_j^e)^{-T}\mathbf{R}_j^e \tag{49}$$

and

$$\bar{\boldsymbol{\phi}}^e = \begin{Bmatrix}\boldsymbol{\phi}_i^e\\ \boldsymbol{\phi}_n^e\end{Bmatrix}. \tag{50}$$

The matrix $\bar{\mathbf{K}}^e$ is symmetrical.

Setting the first variation of Π_p with respect to $\bar{\boldsymbol{\phi}}^e$ to zero gives

$$\sum_e (\bar{\mathbf{K}}^e\bar{\boldsymbol{\phi}}^e - \bar{\mathbf{R}}^e) = \mathbf{0}. \tag{51}$$

Equation (51) represents the stiffness equations for the elements in the region. Assembly and solution of the element equations follows standard finite element procedures. Only slight modifications are required to account for the variable element degrees of freedom.

With the elimination of the normal stress variables, the final variables are displacement parameters only. The elements are non-conforming other than at corners. As the number of terms in $\boldsymbol{\phi}_n^e$ is increased, the discontinuities in normal displacements between adjacent elements tend to zero. Hence as M^* tends to infinity the elements become conforming, with continuity of displacements throughout.

EXAMPLES

Two examples are considered to demonstrate the performance of the proposed element. The boundary conditions in the figures below are indicated by the symbols S (simple support), C (clamped support) and F (free edge).

Example 1

Figure 4 shows a beam of dimensions $L \times D$ which is simply supported along the vertical sides and free on the horizontal sides. It is subjected to a constant body load, $\bar{b}_y$, in the y direction. An exact solution for this problem can be derived in the form of an infinite series using the approach of [9]. Taking symmetry into account, a quarter of the beam was analysed using a uniform mesh of $N_x \times N_y$ elements. Poisson's ratio was taken as 0.3.

Results using a simple element and taking $L/D = 1$ are given in Tables 1 and 2. Convergence to the exact solution is achieved as M and M^* approach infinity. Convergence is not monotonic as the original element variables are mixed. The tables show that good convergence is generally achieved when $M^* \geqslant M$. Increasing M for a given M^* is generally a poor

Table 1. Example 1: ratio of approximate to exact vertical displacement at point 1 ($L/D = 1, N_x = N_y = 1$)

	M					
M^*	1	2	3	4	5	10
1	0.976	0.985	0.995	1.002	1.008	1.025
2	0.993	0.995	0.996	0.997	0.997	0.998
3	0.998	0.998	0.999	0.999	0.999	0.999
4	0.999	0.999	0.999	0.999	1.000	1.000
5	1.000	1.000	1.000	1.000	1.000	1.000
10	1.000	1.000	1.000	1.000	1.000	1.000

Table 2. Example 1: ratio of approximate to exact horizontal stress at point 1 ($L/D = 1$, $N_x = N_y = 1$)

	M					
M^*	1	2	3	4	5	10
1	0.591	0.401	0.276	0.207	0.163	0.074
2	0.926	0.906	0.857	0.840	0.825	0.805
3	0.977	0.998	0.966	0.966	0.958	0.952
4	0.988	1.015	0.985	0.990	0.983	0.980
5	0.994	1.021	0.991	0.999	0.990	0.989
10	1.006	1.025	0.997	1.007	0.997	0.999

Table 3. Example 1: ratio of approximate to exact vertical displacement and horizontal stress at point 2 ($L/D = 1$, $N_x = N_y = 1$)

$M = M^*$	Disp.	Stress
1	1.018	1.017
2	1.001	0.999
3	1.000	1.000
4	1.000	1.000
5	1.000	1.000

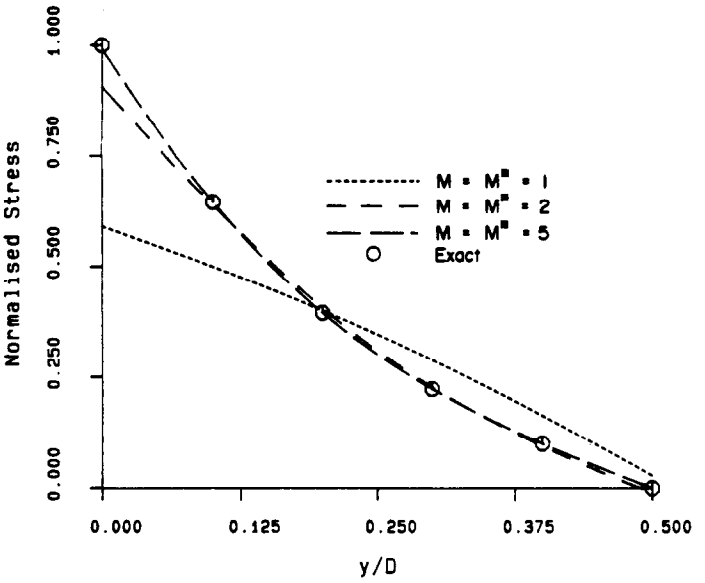

Fig. 5. Example 1: horizontal stress at midspan ($L/D = 1$, $N_x = N_y = 1$).

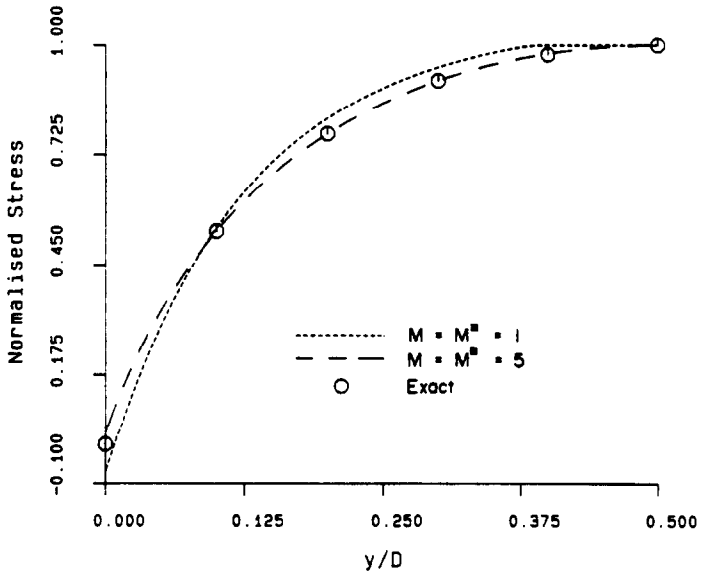

Fig. 6. Example 1: shear stress at $x = 0$ ($L/D = 1$, $N_x = N_y = 1$).

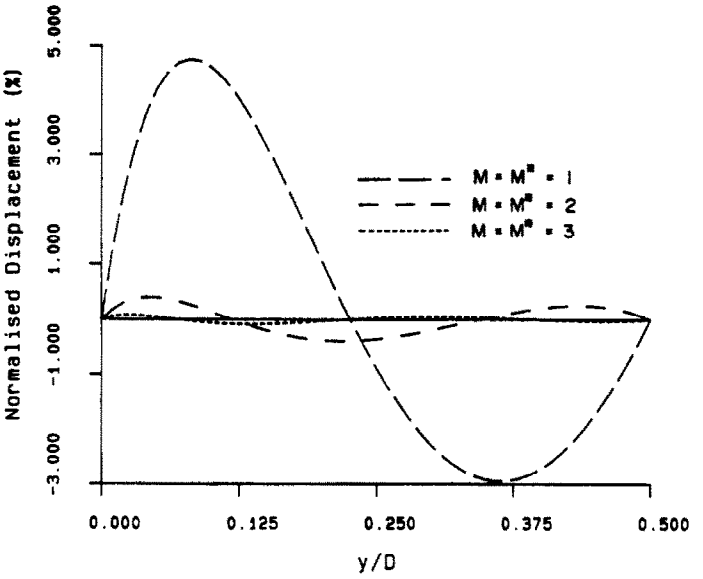

Fig. 7. Example 1: horizontal displacement at midspan ($L/D = 1, N_x = N_y = 1$).

strategy. Although the order of the approximation of the tangential displacements increases, the discontinuities in normal displacements are not reduced. Hence, errors are still present in the solution. To limit the total degrees required in practice, the use of $M = M^*$ is recommended. Convergence is rapid for both the displacement and stress for this combination.

As noted previously, the assumed element displacement functions satisfy the governing differential equations [eqn. (1)]. Therefore, it should be expected that convergence be more rapid in element interiors than on element boundaries based on St Venant's principle. This is demonstrated in Table 3, where the displacement and stress at the centre of the macro element are shown for varying values of $M = M^*$. Convergence is rapid with almost negligible errors for $M = M^* = 2$.

The horizontal stress at midspan is shown in Fig. 5. Convergence is rapid with negligible errors when $M = M^* = 5$. The shear stress at $x = 0$ is also accurately determined, as shown in Fig. 6.

The horizontal displacement and shear stress at midspan are theoretically zero. The horizontal displacement can be exactly set to zero at the corners of the element corresponding to the points $(L/2, 0)$ and $(L/2, D/2)$. In addition, weighted integrals of the horizontal displacement are set to zero as M^* is increased. As M^* increases, the amplitude of the displacement decreases and the curve oscillates with increased frequency about zero, as shown in Fig. 7.

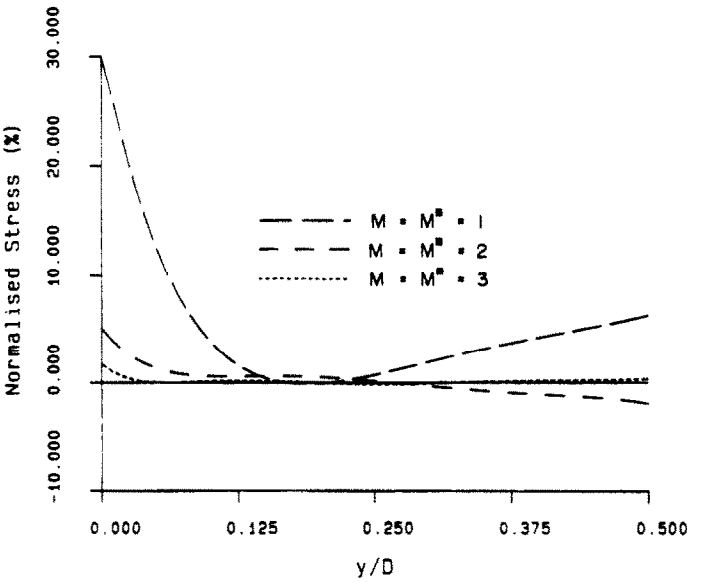

Fig. 8. Example 1: shear stress at midspan ($L/D = 1, N_x = N_y = 1$).

Table 4. Example 1: ratio of approximate to exact vertical displacement and horizontal displacement at point 1 ($N_x = N_y = 1$)

(a) Vertical displacement

	L/D			
$M = M^*$	1	2	5	10
1	0.976	0.993	0.999	1.000
2	0.995	0.999	1.000	1.000
3	0.999	1.000	1.000	1.000
4	1.000	1.000	1.000	1.000
5	1.000	1.000	1.000	1.000
10	1.000	1.000	1.000	1.000

(b) Horizontal stress

	L/D			
$M = M^*$	1	2	5	10
1	0.591	0.874	0.995	1.008
2	0.906	1.007	1.014	1.014
3	0.966	0.997	1.003	1.004
4	0.990	1.005	1.005	1.004
5	0.990	0.999	1.002	1.002
10	0.999	1.001	1.001	1.001

Table 5. Example 1: ratio of approximate to exact vertical deflection and horizontal stress at point 1 ($L/D = 1$)

$N_x = N_y$	$M = M^*$	DOF	Disp.	Stress
1	1	20	0.976	0.591
	2	28	0.995	0.906
	3	36	0.999	0.996
	4	44	0.999	0.990
	5	52	1.000	0.990
	10	92	1.000	0.999
2	1	54	0.993	0.541
	2	78	0.999	0.975
	3	102	1.000	0.994
	4	126	1.000	0.997
	5	150	1.000	0.998
3	1	104	0.996	0.553
	2	152	1.000	0.988
	3	200	1.000	0.998
	4	248	1.000	0.998
	5	296	1.000	0.999

Table 6. Results for example 2

$M = M^*$	Ev_1/P	$L\sigma_{xx2}/P$
1	115.0	9.017
2	115.1	8.944
3	115.2	9.047
4	115.2	9.043
5	115.2	8.966
10	115.2	8.982
Beam theory	115.2	9.000

The condition of zero shear stress at midspan is a natural boundary condition. Hence, the shear stress cannot be exactly set to zero at midspan and it tends to zero only in the limit as the number of series terms is increased. As M and M^* increase, the amplitude of the shear stress decreases and the curve oscillates with increased frequency about zero, as shown in Fig. 8.

The influence of the element aspect ratio, L/D, on the accuracy of the element is shown in Table 4. It can be seen from the table that the accuracy of the elements does not deteriorate significantly as the aspect ratio is increased, although more series terms are required. This confirms that large elements may be used without significant accuracy penalty, unlike conventional finite elements.

The effect of mesh refinement on the results is shown in Table 5. It can be seen that mesh refinement does not improve the performance. This is probably due to errors at element interfaces being introduced with mesh refinement. With single elements, internal errors do not occur as the governing differential equations are satisfied. Hence, using the minimum number of macro elements possible is a simple and effective strategy to adopt. The tables also show that the results for $M = M^* = 1$ are greatly inferior to the results for M and $M^* > 1$. Hence, it is recommended that a minimum of two series terms be used in all cases.

Example 2

A cantilever beam subjected to a parabolic end shear, P, as shown in Fig. 9, was analysed. There is no exact solution for this problem as the completely fixed boundary causes a stress singularity at point 3 and at point 4. Due to symmetry, only the top half of the beam was analysed using a single element. Poisson's ratio was taken as 0.3. Table 6 gives results for the vertical deflection at point 1 and the horizontal stress at point 2 which are compared with the results from beam theory including shear deformation. Again, convergence is rapid, with few degrees of freedom required to achieve engineering accuracy.

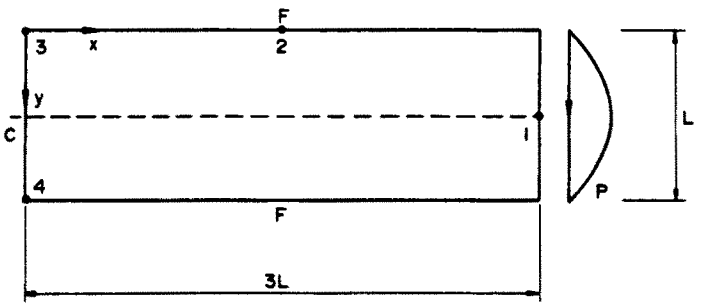

Fig. 9. Example 2: cantilever beam subjected to end shear force.

CONCLUSIONS

The proposed macro element enables the accurate solution of two-dimensional stress problems using few degrees of freedom. The formulation is in terms of displacement variables only, enabling the element to be easily coupled with an analogous plate bending element. Large elements may be used, requiring a minimum of data preparation. Convergence is readily assessed by increasing the number of series terms, avoiding the necessity of defining a new mesh. Engineering accuracy is obtained for both displacements and stresses with few degrees of freedom.

REFERENCES

1. H. C. Chan and Y. K. Cheung, Analysis of shear walls using higher order finite elements. *Build. Envir.* **14**, 217–224 (1979).
2. H. V. Advai, Rectangular finite elements in deep beam problems. *J. Struct. Engng* **4**, 85–88 (1976).
3. J. Petrolito and B. W. Golley, Plate bending analysis using macro elements. *Comput. Struct.* **28**, 407–419 (1988).
4. J. Petrolito, Macro elements in stress analysis. Ph.D. thesis, Department of Civil Engineering, University College, University of New South Wales (1986).
5. B. W. Golley and J. Petrolito, A combined boundary element–macro element method for torsion analysis. In *1st Boundary Element Technology Conf.: BETECH 85* (Edited by C. A. Brebbia and B. J. Noye), pp. 11–17. Springer, Berlin (1985).
6. B. W. Golley and J. Petrolito, Combined finite element–macro element solutions of Helmholtz's equation. In *Computational Techniques and Applications Conf.: CTAC 85* (Edited by B. J. Noye), pp. 273–284. North-Holland, Amsterdam (1986).
7. S. P. Timoshenko and J. N. Goodier, *Theory of Elasticity*, 3rd Edn. McGraw-Hill, New York (1970).
8. N. I. Muskhelishvili, *Some Basic Problems of the Mathematical Theory of Elasticity*, Noordhoff, Groningen (1953).
9. J. E. Goldberg and H. E. Leve, Theory of prismatic folded plate structures. *IABSE Publ.* **27**, 59–86 (1957).

APPENDIX

Terms in $\mathbf{P}$ *and* $\bar{\mathbf{P}}$

$$\mathbf{P} = \lfloor 1, 0, x, 0, 0, x^2, y^2, -c_2xy, -c_1xy, y^3 - c_5x^2y, c_6x^2y \rfloor$$

$$\bar{\mathbf{P}} = \lfloor 0, 1, 0, 0, x, y, -c_1xy, -c_2xy, x^2, y^2, c_6xy^2, x^3 - c_5xy^2 \rfloor,$$

where $c_1 = 4/(1+\nu)$, $c_2 = 2(1-\nu)/(1+\nu)$, $c_3 = 1.5(1-\nu)/\nu$, $c_4 = 1.5(1+\nu)/\nu$, $c_5 = 6/(3+\nu)$ and $c_6 = 3(1+\nu)/(3+\nu)$.

Polynomial shape functions

$$\begin{aligned}\mathbf{N}_p = \lfloor & f_2(b-y, a-x, b, a),\ f_1(a-x, b-y, a, b),\\ & f_3(x, b-y, a, b),\ f_2(b-y, x, b, a),\\ & -f_1(x, b-y, a, b),\ -f_4(b-y, x, b, a),\\ & f_2(y, x, b, a),\ f_1(x, y, a, b),\ f_3(x, y, a, b),\\ & f_2(y, a-x, b, a),\ -f_1(a-x, y, a, b),\\ & f_4(b-y, a-x, b, a)\rfloor\end{aligned}$$

$$\begin{aligned}\bar{\mathbf{N}}_p = \lfloor & f_1(b-y, a-x, b, a),\ f_2(a-x, b-y, a, b),\\ & -f_4(x, b-y, a, b),\ -f_1(b-y, x, b, a),\\ & f_2(x, b-y, a, b),\ f_3(b-y, x, b, a),\\ & f_1(y, x, b, a),\ f_2(x, y, a, b),\\ & f_4(x, y, a, b),\ -f_1(y, a-x, b, a),\\ & f_2(a-x, y, a, b),\ f_3(b-y, a-x, b, a)\rfloor,\end{aligned}$$

where

$$f_1(x, y, a, b) = \frac{y(1+\nu)(4y+b)(b-y)}{6ab^2(1-\nu)}$$

$$f_2(x, y, a, b) = \frac{x(3y(1-\nu)(2y-b) + 4(a^2-x^2)}{3ab^2(1-\nu)}$$

$$f_3(x, y, a, b) = \frac{4y(3x(a-x)(1-\nu) - 2(b^2-y^2)}{3a^2b(1-\nu)}$$

$$f_4(x, y, a, b) = \frac{2x(a-2x)(a-x)}{3a^2b(1-\nu)}.$$

Series shape functions

$$\begin{aligned}\mathbf{N}_{im} = \lfloor & f_{m1}(x, b-y, a, b, m),\ f_{m2}(y, x, b, a, m),\\ & f_{m1}(x, y, a, b, m),\ -f_{m2}(y, a-x, b, a, m)\rfloor\end{aligned}$$

$$\begin{aligned}\bar{\mathbf{N}}_{im} = \lfloor & -f_{m2}(x, b-y, a, b, m),\ f_{m1}(y, x, b, a, m),\\ & f_{m2}(x, y, a, b, m),\ f_{m1}(y, a-x, b, a, m)\rfloor,\end{aligned}$$

where

$$\begin{aligned}f_{m1}(x, y, a, b, m) = \frac{\cos(\alpha_m x)}{2s^2}[& s\alpha_m y(1+\nu)\cosh(\alpha_m y)\\ & + 2s\sinh(\alpha_m y)\\ & - \alpha_m b(1+\nu)\cosh(\alpha_m b)\sinh(\alpha_m y)]\end{aligned}$$

$$\begin{aligned}f_{m2}(x, y, a, b, m) = \frac{\sin(\alpha_m x)}{2s^2}\Bigg[& \alpha_m b(1+\nu)\\ & \times\left(\frac{y}{b}s\sinh(\alpha_m y) - c\cosh(\alpha_m y)\right)\\ & - (1-\nu)s\cosh(\alpha_m y)\Bigg].\end{aligned}$$

In the above formulae,

$$s = s(a, b, m) = \sinh(\alpha_m b), \quad c = c(a, b, m) = \cosh(\alpha_m b)$$

and

$$\alpha_m = \alpha_m(a, m) = m\pi/a.$$

$$\begin{aligned}\mathbf{N}_{nm} = \lfloor & f_{m3}(x, b-y, a, b, m)/h,\ f_{m4}(y, x, b, a, m)/h\\ & f_{m3}(x, y, a, b, m)/h,\ -f_{m4}(y, a-x, b, a, m)/h\rfloor\end{aligned}$$

$$\begin{aligned}\bar{\mathbf{N}}_{nm} = \lfloor & -f_{m4}(x, b-y, a, b, m)/h,\ f_{m3}(y, x, b, a, m)/h,\\ & f_{m4}(x, y, a, b, m)/h,\ f_{m3}(y, a-x, b, a, m)/h\rfloor,\end{aligned}$$

where

$$f_{m3}(x, y, a, b) = \frac{\cos(\alpha_m x)(1+\nu)^2 b}{2Es^2} \times \left[c \sinh(\alpha_m y) - \frac{y}{b} s \cosh(\alpha_m y) \right]$$

$$f_{m4}(x, y, a, b, m) = \frac{\sin(\alpha_m x)(1+\nu)}{2E\alpha_m s^2} [\alpha_m b(1+\nu)c \cosh(\alpha_m y) - \alpha_m y(1+\nu)s \sinh(\alpha_m y) + (3-\nu)s \cosh(\alpha_m y)].$$

Transformation matrix

$$\mathbf{T}_m = \begin{bmatrix} 1 & 0 & 0 & 0 \\ 0 & 0 & 0 & 1 \\ (-1)^m & 0 & 0 & 0 \\ 0 & 1 & 0 & 0 \\ 0 & 0 & (-1)^m & 0 \\ 0 & (-1)^m & 0 & 0 \\ 0 & 0 & 1 & 0 \\ 0 & 0 & 0 & (-1)^m \end{bmatrix}$$